

StarFT: Robust Fine-tuning of Zero-shot Models via Spuriousity Alignment

Younghyun Kim^{1*} Jongheon Jeong^{2*} Sangkyung Kwak³
 Kyungmin Lee⁴ Juho Lee⁴ Jinwoo Shin⁴

¹Samsung ²Korea University ³General Robotics ⁴KAIST

yh990220.kim@samsung.com jonghj@korea.ac.kr

sangkyung.kwak@generalrobotics.company {kyungmnlee, juholee, jinwoos}@kaist.ac.kr

Abstract

Learning robust representations from data often requires scale, which has led to the success of recent zero-shot models such as CLIP. However, the obtained robustness can easily be deteriorated when these models are fine-tuned on other downstream tasks (*e.g.*, of smaller scales). Previous works often interpret this phenomenon in the context of domain shift, developing fine-tuning methods that aim to preserve the original domain as much as possible. However, in a different context, fine-tuned models with limited data are also prone to learning features that are spurious to humans, such as background or texture. In this paper, we propose StarFT (Spurious Textual Alignment Regularization), a novel framework for fine-tuning zero-shot models to enhance robustness by preventing them from *learning spuriousity*. We introduce a regularization that aligns the output distribution for spuriousity-injected labels with the original zero-shot model, ensuring that the model is not induced to extract irrelevant features further from these descriptions. We leverage recent language models to get such spuriousity-injected labels by generating alternative textual descriptions that highlight potentially confounding features. Extensive experiments validate the robust generalization of StarFT and its emerging properties: zero-shot group robustness and improved zero-shot classification. Notably, StarFT boosts both worst-group and average accuracy by 14.30% and 3.02%, respectively, in the Waterbirds group shift scenario, where other robust fine-tuning baselines show even degraded performance.¹

1 Introduction

Large-scale vision-language models [Radford et al., 2021, Jia et al., 2021, Zhai et al., 2023] pre-trained on massive image-caption pairs are shown to have rich representations that generalize to a wide range of tasks, even without fine-tuning on task-specific data (*i.e.*, zero-shot generalization).

^{*}Equal contribution

¹Code is available at <https://github.com/alinlab/StarFT>.

These zero-shot models, such as CLIP [Radford et al., 2021], have demonstrated impressive performance on diverse downstream tasks (defined by a set of textual prompts) without any fine-tuning on a specific target dataset. More intriguingly, zero-shot models are further reported to achieve unprecedented robustness across a range of benchmarks involving distribution shifts, which have been a major challenge in the literature [Taori et al., 2020, Miller et al., 2021]. This suggests that the ability to generalize on “out-of-distribution” (OOD) inputs may be an emergent property at scale of data.

Although existing zero-shot models provide reasonable performance on diverse tasks, one is often tempted to further *fine-tune* the models in practice when there are task-specific data available to improve their in-distribution (ID) performance. While such fine-tuning methods effectively enhance ID performance, they are also known to compromise the OOD robustness of the original zero-shot models [Bommasani et al., 2022, Wortsman et al., 2022]. As such, efforts have been recently made to understand the underlying causes of degradation in OOD robustness and mitigate the issue, which is referred to as *robust fine-tuning*. For example, Goyal et al. [2023] have shown that aligning fine-tuning objective with the pre-training stage can improve robustness, and several other works have introduced additional regularization terms [Mao et al., 2022a, Nushi et al., 2018].

However, in a broader context, the lack of model robustness is often attributed to learning *spurious features* [Geirhos et al., 2020, Jaini et al., 2024, Wichmann and Geirhos, 2023], *i.e.*, features that are not aligned with human decision-making but are present in the training data: *e.g.*, background [Xiao et al., 2021], texture [Geirhos et al., 2019], and resolution [Touvron et al., 2019]. Existing robust fine-tuning approaches overlook this contributing factor that fine-tuned models depend on confounding decision rules. As it is likely that existing zero-shot models and their fine-tuned derivatives also possess certain types of spuriousity that may affect their robustness, further research has been demanded to explore and address them, particularly in the context of broader OOD robustness benchmarks.

Contribution. Motivated by this, we aim to interpret the degradation in OOD robustness of zero-shot models by focusing on the notion of *spuriousity*. We guide fine-tuned models to avoid constructing unnecessary decision rules so that the models are more closely aligned with human decision

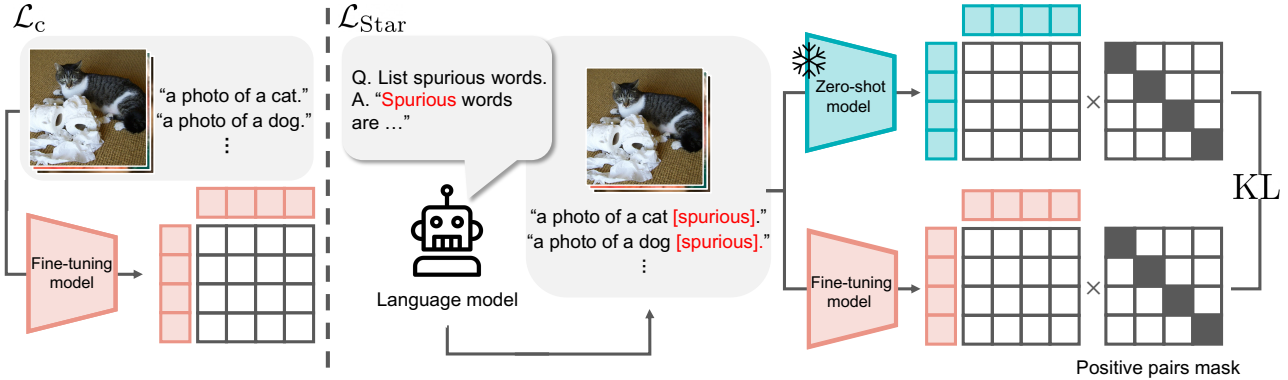


Figure 1: **Overview of StarFT.** Aside from the base contrastive objective \mathcal{L}_c , we propose a novel spuriousity textual alignment regularization $\mathcal{L}_{\text{Star}}$. We first extract spurious textual descriptions from language model, and corrupt the label textual descriptions. We then prevent fine-tuned models from learning spuriousity by minimizing the KL divergence of negative pairs’ corrupted textual descriptions.

making, which results in improved OOD robustness across diverse benchmarks. We mitigate the models’ reliance on spuriousity by specifying irrelevant textual descriptions that they should not learn during fine-tuning. We identify the confounding features, such as background, with the aid of language models (LMs).

Specifically, we propose *Spurious Textual Alignment Regularization* (StarFT), a novel framework tackling spuriousity for robust fine-tuning of zero-shot models, *e.g.*, CLIP. We generate spurious textual descriptions by querying LMs using only general information, such as “image classification,” without any other task-specific prompts, requiring no additional efforts to construct prompts. Then, we inject the obtained textual spuriousity into the label textual descriptions and regularize fine-tuned models to align the logits distribution of corrupted textual descriptions with zero-shot models. By directly providing spurious cues to the models and preventing models from extracting such cues during the fine-tuning process, we retrieve the obtained robustness of large-scale pre-trained zero-shot models.

We show that StarFT enhances various aspects of zero-shot models: OOD robustness, group shift robustness, zero-shot classification, and transfer learning. Although devising an advanced fine-tuning method for CLIP is a popular research topic recently, there exists no such “universally-good” method in the literature to the best of our knowledge.

Our contributions are:

- From the observation that fine-tuned models learn spuriousity (Section 3.1), we propose a novel regularization loss that enforces fine-tuned models not to learn the spuriousity (Section 3.2).
- We demonstrate that spuriousity textual alignment has indeed improve OOD robustness, as supported by our experiments in domain shift benchmarks (Section 4.1).
- We also explore the application of spuriousity textual alignment, achieving zero-shot group robustness (Section 4.2); StarFT demonstrates group robustness in the Waterbirds dataset without having seen any Waterbirds data, where background bias is artificially injected.

- Finally, we show that our method enjoys a broader usage by applying it to zero-shot classification (Section 4.3) and transfer learning scenarios (Section 4.4).

2 Related Work

Out-of-distribution generalization. To deploy machine learning models for real-world applications, the generalization ability to unseen data distribution is crucial [Wiles et al., 2022]. To remedy the performance degradation under distribution shifts, extensive efforts have been proposed to enhance the performance under benchmarks that focus on evaluating robustness [Torralba and Efros, 2011, Recht et al., 2019, Hendrycks et al., 2020, Shankar et al., 2020, Hendrycks et al., 2021a, Tramèr and Boneh, 2019, Paul and Chen, 2021, Mao et al., 2022b, Wang et al., 2021]. Prior works aim to increase OOD robustness by training with sophisticated data augmentations [Hendrycks et al., 2020, 2021a], adversarial training [Tramèr and Boneh, 2019], using advanced network architecture [Paul and Chen, 2021, Mao et al., 2022b] or extra information from test-time samples [Wang et al., 2021]. Despite the tremendous efforts, there still exists a clear gap between the ID and OOD accuracy [Miller et al., 2021]. Recent works on zero-shot models [Radford et al., 2021, Jia et al., 2021, Zhai et al., 2023] have shown that the existing gap between ID and OOD performance can be notably reduced by scaling up the data curation, demonstrating large improvements in various robustness benchmarks. Our work is based upon these advances, by focusing on robust fine-tuning of recent zero-shot models.

Robust fine-tuning of zero-shot models. Motivated by the fact that fine-tuning zero-shot models is often at the cost of OOD generalization [Andreassen et al., 2021, Kumar et al., 2022, Wortsman et al., 2022], various works have explored techniques to preserve the robustness of the zero-shot model while improving its ID accuracy [Li et al., 2018, Wortsman et al., 2022, Kumar et al., 2022, Tian et al., 2023, Goyal et al., 2023, Mao et al., 2022a, Nam et al., 2024, Oh et al., 2024, Choi et al., 2024]. Overall, they have studied post-hoc approaches [Wortsman et al., 2022, Tian et al., 2023], training

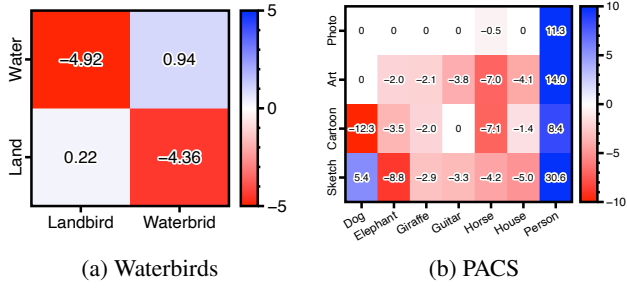


Figure 2: **Subgroup accuracies in group shift benchmarks.** Differences of subgroup accuracies (%) between zero-shot and FLYP fine-tuned models.

schemes [Kumar et al., 2022, Goyal et al., 2023, Choi et al., 2024], and regularization schemes [Mao et al., 2022a, Nam et al., 2024, Oh et al., 2024] to better preserve the zero-shot model as prior knowledge. For instances, WiSE-FT [Wortsman et al., 2022] considers a weight ensembling between the zero-shot and fine-tuned models, and Tian et al. [2023] have proposed a projection of the fine-tuned weights to be close to the zero-shot model; both in a post-hoc manner. FLYP [Goyal et al., 2023] has shown that aligning fine-tuning objective with those of the pre-training stage can improve the OOD performance; AutoFT [Choi et al., 2024] considers a bi-level optimization to search for a fine-tuning objective based on small OOD validation data; CAR-FT [Mao et al., 2022a] regularizes context distributions induced by zero-shot and fine-tuned models, Lipsum-FT [Nam et al., 2024] reduces energy gap using random texts, and CaRot [Oh et al., 2024] adds self-distillation regularization.

3 Method

We propose StarFT, a robust fine-tuning method leveraging the spurious concept. Our motivation stems from the weakness of naïve fine-tuning objective in Section 3.1 and we explain the proposed method in Section 3.2. Our goal is to enhance generalization ability of fine-tuned models to OOD domains without compromising ID domain performance. Given a foundation model and a set of spurious concepts, StarFT regularizes models to avoid extracting spurious features other than label information, *i.e.*, “[class],” to preserve the robustness of the pre-trained foundation model.

Throughout the paper, we consider an open vocabulary image classification task, where the goal is to map an image $I \in \mathcal{I}$ to a label $y \in \mathcal{Y}$ using image-text aligned vision language models like CLIP [Radford et al., 2021]. Given image-label pairs, we design label textual description $T \in \mathcal{T}_y$ of image I using templates such as “a photo of a [class]” with class names of each label y .

3.1 Motivation

Contrastive loss for fine-tuning. We start by considering a fine-tuning of the CLIP [Radford et al., 2021] model on a labeled image dataset, specifically using contrastive loss as done in FLYP [Goyal et al., 2023]. A typical practice for fine-tuning CLIP is to minimize cross-entropy loss; *viz.*, it initial-

izes a new linear head upon the CLIP image embedding to define logits, discarding the textual labels of a given dataset. Therefore, the fine-tuned model is no longer suitable for open vocabulary tasks. In contrast, employing contrastive loss enables the fine-tuned model to continue processing language inputs as like CLIP. Formally, given a batch of N image-text pairs $\mathcal{B} = \{(I_i, T_i)\}_{i=1}^N$, let us denote $\mathbf{f}_\theta : \mathcal{I} \rightarrow \mathbb{R}^d$ an image encoder and $\mathbf{g}_\theta : \mathcal{T} \rightarrow \mathbb{R}^d$ a text encoder. Then the contrastive loss is given as follows:

$$\mathcal{L}_C(\theta; \mathcal{B}) = -\frac{1}{2N} \sum_{i=1}^N \left(\log \frac{e^{\mathbf{x}_i \cdot \mathbf{y}_i / \tau}}{\sum_{j=1}^N e^{\mathbf{x}_i \cdot \mathbf{y}_j / \tau}} + \log \frac{e^{\mathbf{x}_i \cdot \mathbf{y}_i / \tau}}{\sum_{j=1}^N e^{\mathbf{x}_j \cdot \mathbf{y}_i / \tau}} \right), \quad (1)$$

where $\mathbf{x}_i = \frac{\mathbf{f}_\theta(I_i)}{\|\mathbf{f}_\theta(I_i)\|_2}$ and $\mathbf{y}_i = \frac{\mathbf{g}_\theta(T_i)}{\|\mathbf{g}_\theta(T_i)\|_2}$ are ℓ_2 -normalized image and text embeddings, and $\tau > 0$ is a temperature. When applied for fine-tuning, it first transforms the class labels of the given dataset into texts using some prompt template, *e.g.*, “a photo of a [class],” and optimizes the contrastive loss (3.1) updating both image and text encoders as well as the temperature τ .

However, it is uncertain whether the contrastive fine-tuning loss truly preserves the original ability of CLIP to associate text prompts to images, especially for prompts beyond the template-based prompts derived from the class labels (used during fine-tuning). To investigate this, we conduct the following group shift experiment asking whether the fine-tuned model retains its ability to handle diverse textual inputs.

Spuriousity in fine-tuned zero-shot models. We discover that although current robust fine-tuning method achieves higher accuracies in both ID and OOD, it also exhibits short-cut learning that learns spurious correlations from biased data [Sagawa et al., 2020, Geirhos et al., 2020] similar to the conventional fine-tuning. To see this, we examine how the subgroup accuracies of a CLIP model change through its fine-tuning (via FLYP) on ImageNet, as shown in Figure 2. We utilize group shift datasets such as Waterbirds [Sagawa et al., 2020] and PACS [Li et al., 2017], where the samples have extra labels indicating their subgroup domains. For example, in Waterbirds, we analyze an ImageNet fine-tuned CLIP using textual prompts such as “a photo of a trench,” and subsequently test it under group shift scenarios with prompts like “a photo of a waterbird in the mountain.” Here, FLYP tends to focus more on confounding features, such as background, rather than the core features, evidenced by its lower performance compared to CLIP on the minor subgroups (*i.e.*, landbirds in water background and waterbirds in land background).

Overall, the results demonstrate that even the most recent advanced robust fine-tuning methods still struggle to avoid spurious correlations during the fine-tuning process. This is an unfavorable behavior, especially since these fine-tuned models are often tested in more challenging conditions, such as real-world scenarios [Geirhos et al., 2020].

3.2 StarFT: Fine-tuning with Spurious Textual Alignment Regularization

Motivated by the observation that fine-tuned zero-shot models show shortcut learning, we prevent the models from

further constructing unnecessary decision rules during fine-tuning. To achieve this, our method, Spurious Textual Alignment Regularization fine-tuning (StarFT), introduces spuriousity suppressing regularization term that restricts model from shortcut learning as illustrated in Figure 1.

Spurious textual alignment regularization. To prevent the model from learning spurious features, *i.e.*, that leads to learning shortcut, we propose a novel fine-tuning objective named *spurious textual alignment regularization*, which uses the spurious descriptors. During fine-tuning with contrastive loss, we construct additional captions that include the spurious words and regularize the output of fine-tuning model with the zero-shot model. In particular, given a batch of N image-text pairs $\mathcal{B} = \{(I_i, T_i)\}_{i=1}^N$, we construct an additional batch $\mathcal{B}_S = \{(I_i, S_i)\}_{i=1}^N$ of image and spuriousity-augmented caption S_i , which is generated by attaching spurious keywords at each T_i . For instance, given the textual description of class name (*e.g.*, “a photo of a [class]”), we uniformly sample a spurious descriptor and augment to the textual description to generate spuriousity-augmented caption (*e.g.*, “a photo of a [class] in the [descriptors]”).

Then, we compute regularization loss by measuring the KL divergence between the softmax outputs of fine-tuning and zero-shot models on \mathcal{B}_S . Specifically, we get the similarities between each image I_i and text S_i using fine-tuning model and zero-shot models. Then, we mask the logits (both fine-tuning and zero-shot) to exclude the pairs that are of same class labels and define q_i to be the softmax probability over the column of masked logits. q_i is given as follows:

$$[q_i]_j = \frac{e^{\mathbf{x}_i \cdot \mathbf{s}_j / \tau}}{\sum_{c(j') \neq c(i)} e^{\mathbf{x}_i \cdot \mathbf{s}_{j'} / \tau}}, \quad (2)$$

where $c(i)$ denotes the class label of I_i , τ is a temperature, and $\mathbf{x}_i = \frac{\mathbf{f}_\theta(I_i)}{\|\mathbf{f}_\theta(I_i)\|_2}$, $\mathbf{s}_j = \frac{\mathbf{g}_\theta(S_j)}{\|\mathbf{g}_\theta(S_j)\|_2}$ are image and text embeddings, respectively. By computing q_i , we represent the relative likelihood of image I_i that is related to the spurious descriptors S_j . Here, we mask out logits from the true class to address cases when zero-shot models perform poorly initially, so that distilling their confidence can be unfavorable: *e.g.*, as shown in Table 9 in Appendix. We define \tilde{q}_i be the softmax over the masked logits of zero-shot models in a similar manner, and compute the spurious textual alignment regularization (Star) loss by KL divergence between q_i and \tilde{q}_i :

$$\mathcal{L}_{\text{Star}}(\theta; \mathcal{B}_S) = \frac{1}{N} \sum_{i=1}^N D_{\text{KL}}(\tilde{q}_i \parallel q_i). \quad (3)$$

Finally, we use linear combination of contrastive fine-tuning loss (*i.e.*, Eq. (3.1)) and Star regularization loss (*i.e.*, Eq. (3)) for fine-tuning, defining the objective of StarFT:

$$\mathcal{L}(\theta; \mathcal{B}, \mathcal{B}_S) = \mathcal{L}_{\text{C}}(\theta; \mathcal{B}) + \lambda_{\text{Star}} \mathcal{L}_{\text{Star}}(\theta; \mathcal{B}_S), \quad (4)$$

where $\lambda_{\text{Star}} > 0$ is a hyperparameter.² This hyperparameter λ_{Star} is linearly decayed during the course of fine-tuning, which helps balancing the tradeoff between ID and OOD accuracy.

²In our experiments, we use $\lambda_{\text{Star}} = 0.5$ by default.

[background]	mountains	beach	desert
[texture]	rough	smooth	soft
[resolution]	blurred	bright	overexposed

Table 1: **Examples of spurious words.** Samples of the obtained spurious words for each spurious concepts. The list of concrete textual descriptions can be found in Appendix C.2.

Obtaining spurious descriptors from LMs. As we leverage language supervision in contrastive learning objective, it is natural to use rich semantics of languages in aligning spuriousity. The advances of large language models have open possibilities of constructing some useful concept banks [Menon and Vondrick, 2023, Oikarinen et al., 2023] or extracting task-specific spurious words [Adila et al., 2024] for classifying images. Motivated by this, we aim to construct a new set of textual concepts that represents spuriousity, regardless of specific domains; see Table 1 for examples. We obtain textual descriptions of spurious concept that models often rely on while making decisions by querying language models. We prompt the LM with the input:

Question: List possible spurious correlations while classifying natural images. Answer in a word.

Answer: 1.

–

Given minimal task description, LMs provide spurious concepts like “background,” “texture,” and “resolution” that corresponds to our belief. Then, to directly corrupt the label textual description T , we ask LMs for more fine-grained spurious descriptors s . For example, for spurious concept “[background],” we get spurious descriptors such as “in the mountains” or “on the beach.” We compose the spurious descriptors set \mathcal{S} for each spurious concept, which is used to corrupt the textual description of an image.

Comparison with other methods. Recent works tackle the robust fine-tuning by introducing additional regularization term, such as CAR-FT [Mao et al., 2022a] and CaRot [Nushi et al., 2018]. CAR-FT optimizes the cross-entropy loss with additional dataset-specific context regularization to guide the fine-tuned model towards the zero-shot model. On the other hand, we regularize spuriousity rather than context, making it scalable to any other datasets. By directly addressing spuriousity, StarFT achieves better robustness than CAR-FT. Also, StarFT integrates with contrastive loss by injecting irrelevant information into the label textual descriptions. This direct adaptation eliminates the computational overhead associated with CAR-FT, which relies on averaged weights of context prompts across classes. CaRot, another recent baseline, optimizes the contrastive loss with additional regularization to maintain the image and textual logit distributions of zero-shot models. Additionally, CaRot updates zero-shot models using an exponential moving average (EMA). Due to this EMA update, CaRot fails on benchmarks where zero-shot models suffer. However, ours does not use EMA update to boost performance, and thus is not affected by whether zero-shot models

Method	ViT-B/16						ViT-L/14					
	IN	IN-R	IN-A	IN-S	IN-V2	Avg.	IN	IN-R	IN-A	IN-S	IN-V2	Avg.
Zeroshot	68.3	77.7	50.0	48.3	61.9	59.5	75.6	87.9	70.8	59.6	69.9	72.0
FT	81.3	71.3	44.5	49.1	71.7	59.1	84.7	75.4	55.7	54.4	75.3	65.2
FLYP	82.6	71.4	48.5	49.8	72.7	60.6	86.2	83.8	68.9	60.2	78.2	72.8
CAR-FT	81.9	75.6	50.0	51.5	72.8	62.5	86.3	84.2	66.6	60.0	76.8	71.9
CaRot	83.1	<u>76.2</u>	<u>51.3</u>	<u>51.9</u>	74.3	63.7	87.0	88.0	72.7	62.7	79.3	75.6
StarFT (Ours)	82.9	77.7	53.7	52.5	73.8	64.4	86.4	88.7	73.8	63.2	78.9	76.1

Table 2: **Evaluation on domain shifts.** We report Top-1 accuracies (%) on ImageNet (IN) and OOD datasets (IN-R, IN-A, IN-S, IN-V2), with their average values (Avg.) for two architectures (ViT-B/16 and ViT-L/14). StarFT outperforms the baselines under domain shifts scenarios on ImageNet. For example, on ViT-B/16, StarFT outperforms full fine-tuning by 5.3% on OOD and 1.6% on IN. We **bold** and underline the top two values in each column.

Method	Waterbirds		PACS		CIFAR-10.02	
	WG	Avg.	WG	Avg.	WG	Avg.
Zeroshot	25.9	87.1	87.4	93.0	47.0	87.0
FT	<u>27.1</u>	85.6	87.6	91.6	62.5	85.7
FLYP	21.5	87.2	86.0	92.5	61.0	88.2
CAR-FT	24.8	86.6	87.2	93.2	<u>63.5</u>	87.3
CaRot	<u>27.1</u>	<u>89.5</u>	<u>88.5</u>	<u>94.2</u>	63.0	<u>89.3</u>
StarFT (Ours)	40.2	90.1	89.1	94.7	64.5	90.2

Table 3: **Evaluation on group shifts.** We report worst-group (WG) and average (Avg.) accuracies (%) of ImageNet fine-tuned models on Waterbirds, PACS, and CIFAR-10.02 datasets. Notably, StarFT (Ours) consistently outperforms baselines including pre-trained CLIP without seeing any data from the group shift benchmarks. We **bold** and underline the top two values in each column.

perform poorly or not.

4 Experiments

First, we demonstrate the robustness of StarFT in diverse distribution shift scenarios (Section 4.1). Then, we present that the model fine-tuned with StarFT is robust to group shift benchmarks (Section 4.2) and outperforms on various object classification datasets (Section 4.3), even outperforming pre-trained zero-shot models. Lastly, we apply StarFT for standard transfer learning tasks (Section 4.4) demonstrating our method’s efficacy in various scenarios.

Baselines. We compare StarFT with various fine-tuning methods for pre-trained zero-shot models; standard fine-tuning with classification loss (FT), and robust fine-tuning approaches such as FLYP [Goyal et al., 2023], CAR-FT [Mao et al., 2022a], and CaRot [Oh et al., 2024].

Implementation details. Throughout experiments, we utilize CLIP [Radford et al., 2021] ViT-B/16 and ViT-L/14 trained on the LAION dataset [Schuhmann et al., 2021] and fine-tune the model using AdamW [Kingma and Ba, 2017] optimizer with a cosine learning rate scheduler. We train models with a batch size of 512 for ImageNet, while all other datasets use a batch size of 256. OOD datasets are only used for evaluation, where we select the best-performing model based on ID validation set accuracy. Across all datasets, we

Method	C-10	C-100	Cal101	STL10	Avg.
	90.8	68.2	89.6	98.3	
Zeroshot	87.7	63.6	85.7	95.3	83.1
FT	90.0	64.2	87.4	98.5	85.0
FLYP	89.7	65.9	88.2	96.7	85.2
CAR-FT	91.1	66.7	89.0	<u>98.7</u>	86.5
StarFT (Ours)	91.4	69.0	89.7	99.0	87.3

Table 4: **Zero-shot evaluation.** We evaluate ImageNet fine-tuned models in different zero-shot scenarios on CIFAR-10 (C-10), CIFAR-100 (C-100), Caltech101 (Cal101), and STL10. Notably, without seen any data from the zero-shot benchmarks, ours consistently outperforms baselines including pre-trained CLIP. We **bold** and underline the top two values in each column.

use the same text-templates as CLIP [Radford et al., 2021] and WiSE-FT [Wortsman et al., 2022]. Further implementation details are in Appendix B.

4.1 Evaluation on domain shifts

Datasets. To assess the performance of our approach across domain shifts, we train StarFT on ImageNet (IN) [Russakovsky et al., 2015], which comprises over a million natural images of 1,000 classes. We then evaluate our fine-tuned models on 4 well-known ImageNet OOD benchmarks: ImageNet-R (IN-R) [Hendrycks et al., 2021a], ImageNet-A (IN-A) [Hendrycks et al., 2021b], ImageNet-Sketch (IN-S) [Wang et al., 2019], and ImageNetV2 (IN-V2) [Recht et al., 2019]. ImageNet-R contains visual renditions such as “cartoons” of ImageNet classes while ImageNet-Sketch contains sketches of ImageNet classes. ImageNet-A consists of naturally occurring samples that are misclassified by ResNet models. ImageNetV2 is a newly curated test set of ImageNet. Each of these variants reflects the domain shift of ImageNet.

Results. As shown in Table 2, StarFT shows the best OOD average accuracy while maintaining high ID accuracy for both small and large CLIP models. This highlights the effectiveness of our spurious alignment loss in enhancing domain robustness, providing empirical evidence that eliminating spuriousity during fine-tuning enhances model robustness against distribution shifts. On ImageNet, with ViT-B/16, our method surpasses full fine-tuning (FT) by 5.3% in OOD av-

Method	Caltech101	Cars	Flowers	ImageNet	iWILD	FMoW	Avg. Rank
Zeroshot	87.7	64.4	81.2	68.3	8.70	20.4	6.0
FT	97.0	84.2	92.4	81.3	45.2	68.6	3.8
FLYP	<u>97.1</u>	89.0	<u>97.1</u>	82.6	<u>48.5</u>	68.6	<u>2.2</u>
CAR-FT	96.1	84.3	94.5	81.9	<u>45.8</u>	<u>68.4</u>	3.7
CaRot	96.0	89.8	95.7	83.1	40.6	51.9	3.3
StarFT (Ours)	97.2	<u>89.5</u>	97.5	<u>82.8</u>	50.1	<u>68.4</u>	1.7

Table 5: **Transfer learning.** We evaluate our proposed approach on 6 different transfer learning datasets. We fine-tune with the downstream datasets and report the ID test accuracy. We **bold** and underline the top two values in each column.

verage accuracy and by 1.57% in ID accuracy. Similarly, with the larger ViT-L/14 architecture, StarFT achieves performance improvements on both ID and OOD datasets. In fact, ours shows the best OOD average accuracy even when compared to baselines with weight ensembling, *i.e.*, via WiSE-FT [Wortsman et al., 2022], as shown in Table 8 in Appendix.

4.2 Evaluation on group shifts

Datasets. We further evaluate our ImageNet fine-tuned models on three different group shift benchmarks: Waterbirds [Sagawa et al., 2020], PACS [Li et al., 2017], and CIFAR-10.02 [Zhang and Ré, 2022]. As we are given the class labels from these datasets, we construct textual descriptions to perform zero-shot evaluations. Waterbirds classifies bird images into landbird and waterbird, with each class has two groups based on the background: bird on land background, and bird on water background. PACS classifies images into 7 categories and each image is from either arts, cartoons, photos or sketches, indicating different groups. CIFAR-10.02 classifies images into 10 categories. We follow Zhang and Ré [2022] to construct CIFAR-10.02, which combines the original CIFAR-10 [Krizhevsky, 2009] and CIFAR-10.2 [Lu et al., 2020] from different data sources, defining each data source as a distinct group.

Results. To verify the effect of our spurious alignment loss in group shifts, which are closely related to spurious correlations, we leverage popular group shift benchmarks as a means of measuring spuriousity. As our objective is to enhance a wide range of robustness by targeting spuriousity, we do not additionally fine-tune with datasets in group shift benchmarks. Since all fine-tuned models are capable of zero-shot classification, we assess the spuriousity inherent in fine-tuned models using zero-shot performance on group shift benchmarks. We report both the worst group accuracy (WG) and the average accuracy (Avg.), as the worst group accuracy reflects the robustness of the model across different groups within the data. Notably, our spurious alignment loss indeed improves the group robustness of the fine-tuned model, resulting in the best WG accuracy among all baselines as depicted in Table 3. It is well known that improving worst group accuracy often comes at the cost of average accuracy [Sagawa et al., 2020]. However, as opposed to this common drawback of eliminating spuriousity, StarFT improves both in the worst group and the average accuracy. This stands out in the Waterbirds benchmark, where ours narrows the gap between the worst group and the average accuracy to 49.88%, which is

61.19% in zero-shot models.

4.3 Zero-shot classification

We also conduct evaluation on zero-shot classification from the ImageNet fine-tuned models on 4 natural image benchmarks: CIFAR-10 [Krizhevsky, 2009], CIFAR-100 [Krizhevsky, 2009], Caltech101 [Li et al., 2022], and STL10 [Coates et al., 2011]. Overall, we observe that StarFT preserves the generalization ability of zero-shot models even after its fine-tuning. As shown in Table 4, StarFT outperforms the baselines including the base zero-shot models, across all datasets considered. In CIFAR-100 and Caltech101, although all fine-tuned baselines show deteriorated zero-shot performance compared to the zero-shot models, ours could maintain or even improve their accuracy.

4.4 Transfer learning

We compare the transferability of StarFT between various fine-tuning methods. We use 6 common object classification datasets: Caltech101 [Li et al., 2022], Stanford-Cars [Krause et al., 2013], Flowers102 [Nilsback and Zisserman, 2008], ImageNet [Russakovsky et al., 2015], WILDS-iWILDCam [Beery et al., 2020, Koh et al., 2021], and WILDS-FMoW [Christie et al., 2018, Koh et al., 2021]. In our experiments, we use the same set of spurious descriptors across datasets. Table 5 shows the results. Compared to a strong baseline such as CaRot [Oh et al., 2024], StarFT (Ours) shows slight degradation on Cars and ImageNet datasets. This is partly due to the CaRot’s EMA update on zero-shot models which iteratively self-distills the knowledge of zero-shot models. However, this approach has drawbacks in scenarios where the zero-shot model performs poorly, such as in WILDS-iWILDCam and WILDS-FMoW. In these datasets, the zero-shot model struggles with ID accuracies of 8.70% and 18.7%, respectively, unlike other datasets. Consequently, CaRot performs significantly worse than other baselines, while StarFT shows consistent improvement across all 6 datasets with the best average rank in transfer learning since ours does not rely on EMA updates.

4.5 Ablation study

Corruption to label textual descriptions. We show the effect of each component in our proposed method in Table 6. We start from adding regularization to FLYP [Goyal et al., 2023] which is the standard contrastive learning objective. Regularizing clean label textual descriptions without any spurious corruptions improves OOD accuracy but degrades the

ImageNet									
$\mathcal{L}_{\text{Star}}$	Suffix	Mask	Decay	IN	IN-R	IN-S	IN-A	IN-V2	Avg.
–	–	–	–	82.6	71.4	48.5	49.8	72.7	60.6
✓	–	–	–	80.4	77.3	51.5	52.4	71.6	63.2
✓	Random	–	–	82.3	77.6	52.4	52.1	73.2	63.8
✓	Spurious	–	–	82.7	78.0	52.8	52.5	73.5	64.2
✓	Spurious	✓	–	82.3	78.2	54.2	52.6	73.3	64.6
✓	Spurious	–	✓	82.9	77.4	53.2	52.3	73.8	64.2
✓	Spurious	✓	✓	82.9	77.7	53.7	52.5	73.8	64.4

Table 6: **Ablation on different components.** We ablate on different parts of StarFT by starting with the baseline, where we regularize the clean label descriptions, and then add random and spurious textual descriptions to corrupt them. Next, we fix to the spurious suffix and examine the effects of other components: masking positive pairs and diminishing regularization ratio.

ImageNet						
Concept	IN	IN-R	IN-S	IN-A	IN-V2	Avg.
[background]	82.9	77.7	53.7	52.5	73.8	64.4
[texture]	82.8	78.3	53.7	53.0	73.8	64.7
[resolution]	82.7	78.3	53.6	53.0	73.8	64.7
all	82.4	78.6	53.9	53.1	73.5	64.8

Table 7: **Ablation on different spurious concepts.** We ablate on different spurious concepts, including “background,” “texture,” “resolution,” and “all.” Adding spurious textual descriptions consistently improves both ID and OOD accuracies.

ID performance as it continues to interfere with learning to fit the in-domain dataset. Then we append the random textual tokens to label textual descriptions to see the effect of spurious descriptions in improvements. Results indicate that adding random tokens in the suffix improves both ID and OOD performance, where adding spurious textual descriptions further boosts the performance.

Component-wise analysis. We further test two additional components of StarFT in Table 6: masking and decaying regularization. For the masking, we observe an overall gain in OOD accuracies on ImageNet, and even larger gains on WILDS-iWILDCam (see Table 9 in Appendix); where there exist many over-confident “wrong” positive pairs (as zero-shot model suffers). Since positive pairs in the mini-batch have very higher confidences than those of negative pairs, it suppresses the model from learning useful knowledge that lies in spurious descriptions, thereby resulting in deterioration of both ID and OOD accuracies. Regarding the decaying regularization; we adopt the decaying λ_{Star} in StarFT primarily due to its effectiveness in preserving ID accuracy. Note that a key practical objective of robust fine-tuning is not only to improve OOD robustness, but also to ensure that ID performance is not compromised. As observed in Table 6, we find that the gain in ID performance (e.g., +0.6% ImageNet accuracy) from the decaying strategy often outweighs the slight drop in OOD robustness (e.g., -0.2% average OOD accuracy). For an additional ablation study, e.g., on the effect of λ , and spuriousity concepts, see Appendix A.

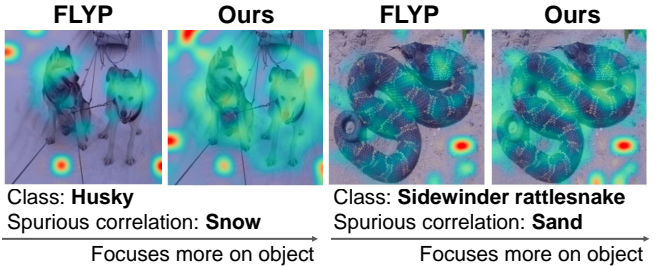


Figure 3: **Mitigation of spuriousity in ImageNet.** We display the GradCAM [Selvaraju et al., 2017] of fine-tuned models for comparison. Each class has the spurious correlations with background such as “snow” in “husky” and “sand” in “rattle snake.” Rather than focusing on mostly background like FLYP, StarFT focuses on object itself to make decisions.

Choice of different spurious concept. By prompting language models, we attain the spurious concept descriptors of “background,” “texture,” and “resolution.” We fine-tune StarFT using each of the spurious concepts and observe that adding spurious descriptions consistently improves both the ID and OOD accuracies. Combination of all concepts results in the slight improvement in OOD accuracy, however, at the cost of ID accuracy, meaning restricting spuriousity too much would sacrifice the ID accuracy. To study the efficacy of our methods in diverse downstream tasks, we fix our spurious concept to “background” throughout the experiments, which shows the best validation ID accuracy. However, we believe that further investigation on combinations of different spurious concepts would be promising research directions.

Spurious correlations in ImageNet. We study the spurious correlations of fine-tuned models in ImageNet. We observe that the StarFT mitigates the spuriousity present in the zero-shot models while classifying ImageNet. To identify the spurious correlations in the zero-shot models, we adopt the setup of Kim et al. [2024] to each of ImageNet classes. We discover that “snow” and “sand” is spuriously correlated to “husky” and “rattle snake,” respectively, indicating a background bias in the zero-shot models. However, this reliance on the background diminishes in StarFT as shown in Figure 3. Compared to ours, the FLYP does not focus on object than background when classifying items.

5 Conclusion

It remains unclear which parts of the knowledge encoded in zero-shot models commit to their effective robustness, and how to preserve it during fine-tuning. We believe our approach of tackling *spuriousity* during fine-tuning suggests a novel view on understanding the robustness of zero-shot models. By devising a textual regularization that aims to prevent models from adopting spurious decision rules, aided by the textual interface of zero-shot models, we could improve the consistency of robustness across many benchmarks, where current methods have been inconsistent. We open the potential of studying the effect of spuriousity in zero-shot model’s fine-tuning on wider notions of robustness. We further discuss on Limitations and Broader impacts in Appendix D.

Acknowledgements

This work was supported in part by Institute of Information & communications Technology Planning & Evaluation (IITP) grant funded by the Korea government(MSIT) (No.RS-2022-II220184, 2022-0-00184, Development and Study of AI Technologies to Inexpensively Conform to Evolving Policy on Ethics) and in part by Center for Applied Research in Artificial Intelligence(CARAI) grant funded by Defense Acquisition Program Administration(DAPA) and Agency for Defense Development(ADD) (UD230017TD). Jongheon Jeong acknowledges support from IITP grants funded by the Korea government (MSIT) (RS-2019-II190079, Artificial Intelligence Graduate School Program (Korea University); IITP-2025-RS-2024-00436857, Information Technology Research Center (ITRC); IITP-2025-RS-2025-02304828, Artificial Intelligence Star Fellowship Support Program to Nurture the Best Talents) and the Korea Creative Content Agency grant funded by the Ministry of Culture, Sports and Tourism (RS-2024-00345025).

References

Alec Radford, Jong Wook Kim, Chris Hallacy, et al. Learning transferable visual models from natural language supervision. In *ICML*, 2021.

Chao Jia, Yinfei Yang, Ye Xia, Yi-Ting Chen, et al. Scaling up visual and vision-language representation learning with noisy text supervision. In *International Conference on Machine Learning*, 2021.

Xiaohua Zhai, Basil Mustafa, Alexander Kolesnikov, and Lucas Beyer. Sigmoid loss for language image pre-training. In *Proceedings of the IEEE/CVF International Conference on Computer Vision*, pages 11975–11986, 2023.

Rohan Taori, Achal Dave, Vaishaal Shankar, Nicholas Carlini, Benjamin Recht, and Ludwig Schmidt. Measuring robustness to natural distribution shifts in image classification. In *Neural Information Processing Systems*, 2020.

John Miller, Rohan Taori, Aditi Raghunathan, Shiori Sagawa, Pang Wei Koh, et al. Accuracy on the line: On the strong correlation between out-of-distribution and in-distribution generalization. In *International Conference on Machine Learning*, 2021.

Rishi Bommasani, Drew A. Hudson, Ehsan Adeli, et al. On the opportunities and risks of foundation models, 2022.

Mitchell Wortsman, Gabriel Ilharco, Jong Wook Kim, Mike Li, et al. Robust fine-tuning of zero-shot models. In *Conference on Computer Vision and Pattern Recognition*, 2022.

Sachin Goyal, Ananya Kumar, Sankalp Garg, Zico Kolter, and Aditi Raghunathan. Finetune like you pretrain: Improved finetuning of zero-shot vision models. In *Conference on Computer Vision and Pattern Recognition*, 2023.

Xiaofeng Mao, Yuefeng Chen, Xiaojun Jia, Rong Zhang, Hui Xue, and Zhao Li. Context-aware robust fine-tuning. *International Journal of Computer Vision*, 2022a.

Besmira Nushi, Ece Kamar, and Eric Horvitz. Towards accountable ai: Hybrid human-machine analyses for characterizing system failure. In *AAAI Conference on Human Computation and Crowdsourcing*, 2018.

Robert Geirhos, Jörn-Henrik Jacobsen, Claudio Michaelis, et al. Shortcut learning in deep neural networks. *Nature Machine Intelligence*, 2(11):665–673, 2020.

Priyank Jaini, Kevin Clark, and Robert Geirhos. Intriguing properties of generative classifiers. In *International Conference on Learning Representations*, 2024.

Felix A. Wichmann and Robert Geirhos. Are deep neural networks adequate behavioral models of human visual perception? *Annual Review of Vision Science*, pages 501–524, 2023.

Kai Xiao, Logan Engstrom, Andrew Ilyas, and Aleksander Madry. Noise or signal: The role of image backgrounds in object recognition. In *International Conference on Learning Representations*, 2021.

Robert Geirhos, Patricia Rubisch, Claudio Michaelis, et al. Imagenet-trained cnns are biased towards texture; increasing shape bias improves accuracy and robustness. In *International Conference on Learning Representations*, 2019.

Hugo Touvron, Andrea Vedaldi, Matthijs Douze, and Hervé Jégou. Fixing the train-test resolution discrepancy. In *Neural Information Processing Systems*, 2019.

Olivia Wiles, Sven Gowal, Florian Stimberg, Sylvestre-Alvise Rebuffi, Ira Ktena, Krishnamurthy Dj Dvijotham, and Ali Taylan Cemgil. A fine-grained analysis on distribution shift. In *International Conference on Machine Learning*, 2022.

Antonio Torralba and Alexei A. Efros. Unbiased look at dataset bias. In *Conference on Computer Vision and Pattern Recognition*, 2011.

Benjamin Recht, Rebecca Roelofs, Ludwig Schmidt, and Vaishaal Shankar. Do imagenet classifiers generalize to imagenet? In *International Conference on Machine Learning*, 2019.

Dan Hendrycks, Norman Mu, Ekin D. Cubuk, et al. Augmix: A simple data processing method to improve robustness and uncertainty. In *International Conference on Learning Representations*, 2020.

Vaishaal Shankar, Rebecca Roelofs, Horia Mania, Alex Fang, Benjamin Recht, and Ludwig Schmidt. Evaluating machine accuracy on ImageNet. In *International Conference on Machine Learning*, 2020.

Dan Hendrycks, Steven Basart, Norman Mu, et al. The many faces of robustness: A critical analysis of out-of-distribution generalization. In *International Conference on Computer Vision*, 2021a.

Florian Tramèr and Dan Boneh. Adversarial training and robustness for multiple perturbations. In *NeurIPS*, 2019.

Sayak Paul and Pin-Yu Chen. Vision transformers are robust learners. In *AAAI*, 2021.

Xiaofeng Mao, Gege Qi, Yuefeng Chen, Xiaodan Li, Ranjie Duan, Shaokai Ye, Yuan He, and Hui Xue. Towards robust vision transformer. In *Neural Information Processing Systems*, 2022b.

Dequan Wang, Evan Shelhamer, Shaoteng Liu, Bruno Olshausen, and Trevor Darrell. Tent: Fully test-time adaptation by entropy minimization. In *International Conference on Learning Representations*, 2021.

Anders Andreassen, Yasaman Bahri, Behnam Neyshabur, and Rebecca Roelofs. The evolution of out-of-distribution robustness throughout fine-tuning, 2021.

Ananya Kumar, Aditi Raghunathan, Robbie Jones, Tengyu Ma, and Percy Liang. Fine-tuning can distort pretrained features and underperform out-of-distribution. In *International Conference on Learning Representations*, 2022.

Xuhong Li, Yves Grandvalet, and Franck Davoine. Explicit inductive bias for transfer learning with convolutional networks. In *ICML*, 2018.

Junjiao Tian, Xiaoliang Dai, Chih-Yao Ma, Zecheng He, Yen-Cheng Liu, and Zsolt Kira. Trainable projected gradient method for robust fine-tuning. In *Conference on Computer Vision and Pattern Recognition*, 2023.

Giung Nam, Byeongho Heo, and Juho Lee. Lipsum-ft: Robust fine-tuning of zero-shot models using random text guidance. In *International Conference on Learning Representations*, 2024.

Changdae Oh, Hyesu Lim, Mijoo Kim, Jaegul Choo, Alexander Hauptmann, Zhi-Qi Cheng, and Kyungwoo Song. Towards calibrated robust fine-tuning of vision-language models, 2024.

Caroline Choi, Yoonho Lee, Annie Chen, Allan Zhou, Aditi Raghunathan, and Chelsea Finn. Autofit: Learning an objective for robust fine-tuning, 2024.

Shiori Sagawa, Pang Wei Koh, Tatsunori B Hashimoto, and Percy Liang. Distributionally robust neural networks for group shifts: On the importance of regularization for worst-case generalization. In *ICLR*, 2020.

Da Li, Yongxin Yang, Yi-Zhe Song, and Timothy M. Hospedales. Deeper, broader and artier domain generalization. In *ICCV*, 2017.

Sachit Menon and Carl Vondrick. Visual classification via description from large language models. In *International Conference on Learning Representations*, 2023.

Tuomas Oikarinen, Subhro Das, Lam M. Nguyen, and Tsui-Wei Weng. Label-free concept bottleneck models. In *International Conference on Learning Representations*, 2023.

Dyah Adila, Changho Shin, Linrong Cai, and Frederic Sala. Zero-shot robustification of zero-shot models. In *International Conference on Learning Representations*, 2024.

Christoph Schuhmann, Richard Vencu, Romain Beaumont, et al. LAION-400m: Open dataset of clip-filtered 400 million image-text pairs, 2021.

Diederik P. Kingma and Jimmy Ba. Adam: A method for stochastic optimization, 2017.

Olga Russakovsky, Jia Deng, Hao Su, et al. Imagenet large scale visual recognition challenge. *International Journal of Computer Vision*, 2015.

Dan Hendrycks, Kevin Zhao, Steven Basart, Jacob Steinhardt, and Dawn Song. Natural adversarial examples. In *CVPR*, 2021b.

Haohan Wang, Songwei Ge, Eric P. Xing, and Zachary C. Lipton. Learning robust global representations by penalizing local predictive power. In *Neural Information Processing Systems*, 2019.

Michael Zhang and Christopher Ré. Contrastive adapters for foundation model group robustness. In *Neural Information Processing Systems*, 2022.

Alex Krizhevsky. Learning multiple layers of features from tiny images, 2009.

Shangyun Lu, Bradley Nott, Aaron Olson, et al. Harder or different? a closer look at distribution shift in dataset reproduction. In *ICML Workshop on Uncertainty and Robustness in Deep Learning*, 2020.

Fei-Fei Li, Marco Andreetto, Marc'Aurelio Ranzato, and Pietro Perona. Caltech 101, 2022.

Adam Coates, Andrew Ng, and Honglak Lee. An analysis of single-layer networks in unsupervised feature learning. In *International Conference on Machine Learning*, 2011.

Jonathan Krause, Michael Stark, Jia Deng, and Li Fei-Fei. 3d object representations for fine-grained categorization. In *IEEE International Conference on Computer Vision Workshops*, pages 554–561, 2013.

Maria-Elena Nilsback and Andrew Zisserman. Automated flower classification over a large number of classes. In *2008 Sixth Indian conference on computer vision, graphics & image processing*, pages 722–729. IEEE, 2008.

Sara Beery, Elijah Cole, and Arvi Gjoka. The iWildCam 2020 competition dataset, 2020.

Pang Wei Koh, Shiori Sagawa, Henrik Marklund, et al. Wilds: A benchmark of in-the-wild distribution shifts. In *International Conference on Machine Learning*, 2021.

Gordon Christie, Neil Fendley, James Wilson, and Ryan Mukherjee. Functional map of the world. In *Conference on Computer Vision and Pattern Recognition*, 2018.

Ramprasaath R. Selvaraju, Michael Cogswell, Abhishek Das, Ramakrishna Vedantam, Devi Parikh, and Dhruv Batra. Grad-CAM: Visual explanations from deep networks via gradient-based localization. In *ICCV*, 2017.

Younghyun Kim, Sangwoo Mo, Minkyu Kim, Kyungmin Lee, Jaeho Lee, and Jinwoo Shin. Discovering and mitigating visual biases through keyword explanation. In *Conference on Computer Vision and Pattern Recognition*, 2024.

Aaron Grattafiori, Abhimanyu Dubey, Abhinav Jauhri, Abhinav Pandey, et al. The Llama 3 herd of models. *arXiv preprint arXiv:2407.21783*, 2024.

OpenAI. Gpt-4 technical report, 2023.

Appendix

A Additional Experiments

Methods	ImageNet						ImageNet					
	w/o ensemble						w/ ensemble					
	IN	IN-S	IN-R	IN-A	IN-V2	Avg.	IN	IN-S	IN-R	IN-A	IN-V2	Avg.
Zeroshot	68.3	77.7	50.0	48.3	61.9	59.5	-	-	-	-	-	-
FT	81.3	70.8	46.4	46.9	71.2	58.8	81.8	75.7	49.8	51.9	72.5	62.5
FLYP	82.6	71.4	48.5	49.8	72.7	60.6	82.9	74.1	51.6	51.3	73.6	62.6
CAR-FT	81.9	75.6	50.5	51.5	72.8	62.5	82.0	77.2	52.0	52.5	72.8	63.6
CaRot	83.1	76.2	51.3	51.9	74.3	63.4	83.1	76.2	51.3	51.9	74.3	63.4
StarFT (Ours)	82.9	77.7	53.7	52.5	73.8	64.4	83.0	78.3	53.0	53.0	73.8	64.5

Table 8: **Weight ensemble results on ImageNet fine-tuned CLIP ViT-B/16.** We report the results based on the ID validation accuracy.

Mask	iWILD	
	ID	OOD
	49.82	34.98
✓	50.09	37.07

Table 9: **Effect of positive pair masking.** We show the effect of masking positive pairs on WILDS-iWILDCam dataset where zero-shot model performs poorly.

Table 10: **Ablation on regularization ratio.** We sweep on $\lambda \in \{0.1, 0.5, 1.0\}$ to see the effect of our regularization ratio to ID and OOD accuracies on ImageNet.

Method	iWILD		FMoW	
	ID	OOD	ID	OOD
Zeroshot	8.70	11.00	20.40	18.70
FT	47.22	35.56	68.64	40.15
FLYP	48.52	36.61	68.56	40.07
CAR-FT	45.75	37.02	68.44	40.69
CaRot	40.61	29.16	51.88	26.80
StarFT (ours)	50.09	37.07	68.41	40.96

Table 11: **Evaluation on additional domain shifts.** Additional results on WILDS-iWILDCam and WILDS FMoW.

ViT-B/16	ImageNet					
	IN	IN-V2	IN-R	IN-A	IN-S	Avg.
Zeroshot	68.3	61.9	77.7	50.0	48.3	59.5
FLYP	82.6	72.7	71.4	48.5	49.8	60.6
StarFT:						
GPT-3.5	82.9	73.8	77.7	53.7	52.5	64.4
Llama-3.3	82.7	73.4	78.1	53.9	52.7	64.5

Table 12: **Ablation on different LM.** Additional results using LLaMA-3.3-70B-Instruct for the concept bank generation.

A.1 Weight ensembling on StarFT

Weight ensembling of fine-tuned models and zero-shot models is a very simple and straightforward method to boost both ID and OOD accuracies. We sweep on different choices of $\alpha \in \{0.0, 0.1, 0.2, 0.3, 0.4, 0.5, 0.6, 0.7, 0.8, 0.9, 1.0\}$ and report the result of weight ensembling selected by the best ID accuracy. As shown in the Table 8, ours show best OOD average accuracy among the baselines. Note that ensembling weight does not improve the ID accuracies of CaRoT and StarFT, as both methods distills beneficial knowledge from zero-shot models that possibly functions like weight ensembling.

A.2 Ablation on spurious regularization ratio

We study the effect of our regularization λ on ID and OOD accuracy. Specifically, we sweep on different choices of $\lambda \in \{0.1, 0.5, 1.0\}$. As expected, if we strengthen our regularization, it improves the OOD accuracy at the cost of ID accuracy.

A.3 Ablation on positive pair mask on WILDS-iWILDCam

As shown in Table 5, the base zero-shot performs poorly on WILDS iWILDCam dataset with ID accuracy of 8.70%. Therefore, distilling the poor-performing zero-shot models' high confidences of true class can negatively affect the fine-tuning procedure. Thus, we mask out logits from the true class (*i.e.*, positive pairs) to address such issue. As shown in Table 9, it shows significant performance drop in OOD accuracy compared to the results with masking.

A.4 Additional domain shifts

We train StarFT on WILDS-iWILDCam [Koh et al., 2021, Beery et al., 2020] and WILDS-FMoW [Koh et al., 2021, Christie et al., 2018]. WILDS-iWILDCam consists of animal images of 182 categories. The ID and OOD datasets are collected from different camera traps, leading to the differences in background, illumination, etc. WILDS-FMoW consists of remote sensing satellite images of 62 categories regarding different locations. The ID and OOD datasets are collected from different geographical sites and time span. StarFT exhibits improved ID and OOD accuracy in iWILDCam and FMoW, showing its efficacy on domain distribution shifts.

A.5 Different language model

We conduct an additional ablation study using a more recent LM, LLaMA-3.3-70B-Instruct [Grattafiori et al., 2024], in the place of GPT-3.5 for the concept bank generation process of StarFT. As shown in Table 12, we observe that spurious descriptions generated by LLaMA-3.3 lead to slightly improved OOD robustness compared to those from GPT-3.5. Nevertheless, StarFT does not exhibit significant degradation even with GPT-3.5, suggesting that it remains robust as long as the language model has a sufficient grasp of spuriousity.

B Experimental Details

B.1 Dataset details

- **ImageNet** [Russakovsky et al., 2015] is a large scale image dataset where the goal is to classify image into one of 1,000 categories. The training set comprises more than million samples, and the validation set comprises 50,000 images (50 images for each class).
- **ImageNetV2** [Recht et al., 2019] is a newly curated text split of ImageNet which comprises the same 1,000 classes as ImageNet.
- **ImageNet-R** [Hendrycks et al., 2021a] is a rendition of ImageNet containing art, cartoons, devianart, graffiti, embroidery, and etc. ImageNet-R has 200 classes of ImageNet.
- **ImageNet-A** [Hendrycks et al., 2021b] collects the samples where ResNet make wrong predictions. ImageNet-A has 200 classes of ImageNet.
- **ImageNet-Sketch** [Wang et al., 2019] contains a sketched version of ImageNet. ImageNet-Sketch has the same 1,000 classe as ImageNet.
- **Waterbirds** [Sagawa et al., 2020] contains 2 different categories of birds: waterbird and landbird. Each image contain two different backgrounds, *i.e.*, water background and land background. Each background serves as a distinct group for group shift evaluation.
- **CIFAR-10.02** [Zhang and Ré, 2022] is a combined dataset from two sources: CIFAR-10 [Krizhevsky, 2009] and CIFAR-10.2 [Lu et al., 2020]. Each category contains images from both source datasets, and the goal is to classify images into one of 10 categories. Each source is treated as a distinct group for group shift evaluation.
- **PACS** [Li et al., 2017] is an image dataset containing 4 different groups: art, painting, cartoon, and sketch. Each group consists of seven categories such as “guitar” and “elephant” and group accuracies are measured for group shift evaluation.
- **CIFAR-10** [Krizhevsky, 2009] is an image dataset containing 10 different categories. The goal is to classify image into one of 10 categories, such as “airplane,” and “dog.”
- **CIFAR-100** [Krizhevsky, 2009] is an image dataset containing 100 different categories, which is a more challenging dataset compared to CIFAR-10. The goal is to classify image into one of 100 categories, such as “airplane,” and “dog.”
- **Caltech101** [Li et al., 2022] contains images of various objects such as “crab” or “mandolin”. The goal is to classify image into one of 101 categories.
- **STL10** [Coates et al., 2011] is an image dataset containing 10 different categories like “airplane”, where the goal is to classify image into one of 10 categories.
- **StanfordCars** [Krause et al., 2013] contains images of cars with different make, model, and year (*e.g.*, 2012 Tesla Model S). The goal is to classify the image into one of 196 categories.
- **Flowers102** [Nilsback and Zisserman, 2008] consists of images of different flowers such as “hibiscus” where the goal is to classify into one of 102 categories.
- **WILDS-iWILDCam** [Beery et al., 2020, Koh et al., 2021] consists of 182 different categories of animal images. To evaluate distribution shift, we split the dataset into ID and OOD based on the camera used and factors like illumination. Models are fine-tuned with only ID dataset and evaluated for OOD datasets.
- **WILDS-FMoW** [Christie et al., 2018, Koh et al., 2021] consists of remote sensing satellite images. We classify satellite images into on of 62 categories, such as “airport” or “zoo”. To evaluate distribution shift, we split the dataset into ID and OOD based on the location and time of their collection. Models are fine-tuned with only ID dataset and evaluated for OOD datasets.

Dataset	Max Epochs	Learning Rate	Weight Decay	Batch Size
Caltech101	100	1e-5	0.0	256
Cars	100	1e-5	0.0	256
Flowers	20	1e-5	0.1	256
ImageNet	10	1e-5	0.1	256
iWILD	20	1e-5	0.2	256
FMoW	20	1e-5	0.2	256

Table 13: **Fine-tuning hyperparameters.**

Dataset	Templates
Waterbirds	“This is a picture of a [class].”
CIFAR-10.02	“a [class].”
PACS	“a [class].”

Table 14: **Prompt design for zero-shot classification.** We use the following prompt design for group shift dataset following Zhang and Ré [2022].

B.2 Training details

We closely follow the training protocols of Goyal et al. [2023] and Wortsman et al. [2022]. All methods, including StarFT, use an AdamW optimizer and cosine learning rate scheduler. A batch size of 512 and regularization ratio λ of 0.5 are applied for ImageNet, while a batch size of 256 and a regularization ratio λ of 0.1 is used for all other datasets. We perform an early stopping based on in-distribution (ID) validation accuracy for all the datasets except ImageNet. For ImageNet, we fine-tune the models for 10 epochs and use them for evaluation. All experiments were run on a machine with 8 NVIDIA V100 GPUs. For fine-tuning CLIP ViT-B/16 on ImageNet, it took approximately 10 hours to run 10 epochs. We list the hyperparameters for each dataset in Table 13.

B.3 Baseline methods

- **Zero-shot (ZS)** [Radford et al., 2021]: Zero-shot classifier is constructed by encoding text descriptions of each class using pretrained CLIP text encoder.
- **Standard Fine-tuning (FT)** [Wortsman et al., 2022]: Starting from the zero-shot linear classification head obtained from pretrained CLIP text encoder, image encoder and linear classifier parameters are fine-tuned with cross-entropy loss.
- **CAR-FT** [Mao et al., 2022a] : CAR-FT regularizes the model during fine-tuning to capture context information alongside the cross-entropy loss. For each dataset, we use prompt templates suggested in FLYP [Goyal et al., 2023] as context prompts, which contains dataset specific information .
- **FLYP** [Goyal et al., 2023] : Both image encoder and text encoder are trained with contrastive loss used to pretrain CLIP [Radford et al., 2021]. In training phase, we use selected template (e.g., “a photo of a [class]”) rather than averaging multiple text description templates.
- **CaRot** [Oh et al., 2024] : CaRoT leverages input-dependant label smoothing obtained by self-distillation using an exponential moving average (EMA) teacher model. We set the hyperparameters regarding EMA update following Oh et al. [2024].

B.4 Prompt templates

Table 14 provides the examples of templates for gorup shift dataset. For all other dataset, we follow the templates from OpenAI³ [Radford et al., 2021].

³https://github.com/openai/CLIP/blob/main/notebooks/Prompt_Engineering_for_ImageNet.ipynb

C Utilization of Language Models

C.1 Prompting language models

We break down our spurious textual description generations into 3 parts. We first get high-level spurious concepts, then we obtain low-level spurious words from these concepts. Finally, we ask for LMs to generate prompt-like spurious descriptions. Specifically, for high-level spurious concept generation, we prompt LMs with:

```
### Your Task ### You are an image classifier classifying a given natural image into a certain class.
```

Question: List possible spurious correlations while classifying natural images. Answer in a word.

Answer: 1.

After we obtain the spurious concept, we ask for more fine-grained spurious words:

```
### Your Task ### You are an image classifier classifying a given natural image into a certain class.
```

Question: List 20 [spurious concept] bias keywords that may lead to a spurious correlation.

Answer: 1.

We prompt GPT-3.5 [OpenAI, 2023] 3 runs for each spurious concept, then remove the duplicated spurious words. Finally, we obtain prompt-like spurious textual descriptions by querying:

```
### Your Task ### You design a proper prompt with a given keyword. The base prompt is "a photo of a [class]." You append an appropriate postfix to the base prompt with the given keyword. You use only one keyword to design each prompt.
```

Question: Design a prompt with following keywords: [keyword1], [keyword2], ...

Answer: 1.

C.2 Spurious textual descriptions

Table 15 provides concrete examples of spurious textual descriptions we obtained via LMs. Specifically, we mainly consider three types of possible spurious concept: “background”, “texture” and “resolution.” Each spurious description is appended as a postfix (or prefix) to the base prompt.

D Discussions

Limitations. Since StarFT tackles general spurious concepts based on the textual descriptions, further investigation into the construction of these spurious concepts is needed. We acknowledge that the hallucination issues in LLMs may affect the effectiveness of our approach. We nevertheless note that our method design can be inherently robust to such issues, given that our objective only regularizes fine-tuning to “not to learn” from the spurious textual embeddings (identified by LLMs): it is still possible to learn from other embeddings even when there are some hallucinated descriptors in the prompt set. This intuition is supported by the consistent performance gains from our experimental validation. However, a deeper assessment of the quality of spurious information would be a promising direction to further boost the effectiveness. We expect that future work can discover and provide guidelines acquiring (or filtering) spurious concepts for specific downstream tasks based on our insights. Also, extending our work to various other of VLMs (*e.g.*, ALIGN [Jia et al., 2021]) beyond CLIP would be an interesting future work.

Broader impact. We argue that understanding capabilities and limitations of foundation models (*e.g.*, CLIP), especially when fine-tuned for specific downstream tasks, is needed. Due to the promising transfer to downstream tasks, individuals may get the sense that these pre-trained models can be successfully applied to any desired downstream tasks. However, our work observes that spuriousity often arises during fine-tuning and highlights the importance of preventing the model to learn undesirable features. Further discussions within this context is needed for better understanding and potential uses of foundation models.

Concept	Spurious descriptions	Concept	Spurious descriptions
Background	“[class] surrounded by flowers”	Texture	“[class] with a rough texture”
	“[class] in urban settings”		“[class] with a smooth surface”
Background	“[class] surrounded by greenery”		“[class] feeling soft to the touch”
	“[class] in snowy landscapes”		“[class] that is hard”
	“[class] in a rainforest”		“[class] with a fuzzy texture”
	“[class] on busy roads and highways”		“[class] with prickly features”
	“[class] in the mountains”		“[class] with a bumpy surface”
	“[class] in parks and gardens”		“[class] appearing fluffy”
	“[class] in front of historical landmarks”		“[class] with silky textures”
	“[class] in fields”		“[class] shining brightly”
	“[class] in the forest and woods”		“[class] with a matte finish”
	“[class] in the snow”		“[class] with wavy patterns”
	“[class] on the beach”		“[class] with knotty features”
	“[class] in a farmland”		“[class] with lumpy textures”
	“[class] on the sand and beach”		“[class] with a sleek appearance”
	“[class] with animals in the frame”	Resolution	“blurred [class]”
	“[class] in entertainment centers”		“blurry [class]”
	“[class] in a suburban area”		“[class] with brightness”
	“[class] under a blue sky”		“dark [class]”
	“[class] surrounded by butterflies”		“distorted [class]”
	“[class] with clouds in the background”		“high resolution of [class]”
	“[class] in cloudy weather”		“low resolution of [class]”
	“[class] in the desert”		“overexposed [class]”
	“[class] among rocks”		“underexposed [class]”
	“[class] in a forest”		“[class] with shadow”
	“[class] in an industrial setting”		“[class] with low visibility”
	“[class] in residential areas”		“[class] with inconsistent lighting”
	“[class] in sports stadiums and arenas”		“cropped [class]”
	“[class] during sunset”		“[class] with cropping”
	“[class] surrounded by trees”		“monochrome [class]”

Table 15: **List of spurious descriptions.** We provide the examples of spurious descriptions obtained using LMs, categorized by spurious concepts (*i.e.*, background, texture, and resolution).